RSC Advances

REVIEW

View Article Online
View Journal | View Issue

Cite this: *RSC Adv.*, 2025, **15**, 26473

Research progress on nanomaterial-empowered electrochemical biosensors for the detection of cardiac troponin I

Ning Zhang,[a] Yuxin Zhu,[b] Fachuang Li,[b] Yusong Wang,[b] Zheng Fu,*[b] Mengda Jia,[b] Xiaoran Zhan[b] and Wanqing Zhang *[b]

Acute myocardial infarction (AMI) is a prevalent and high-risk type of cardiovascular disease (CVD) and a major threat to global human health. Rapid and accurate diagnosis of CVD is important to protect life and health. Cardiac troponin (cTnI) is considered the best biomarker for diagnosing AMI because of its high specificity and sensitivity to acute cardiomyocyte injury. In recent years, electrochemical sensing technology has provided a unique platform for accurate quantitative detection of cardiac biomarkers, effectively shifting early diagnosis of CVD to a higher level of precision and intelligence. Among them, electrochemical biosensors have demonstrated significant potential in monitoring the occurrence and development of CVD due to their benefits including rapid response, high sensitivity, and low cost. This work focuses on the use of various sensing materials including carbon-based materials, metal matrix composites, ceramic matrix composites, MOF composites and conductive polymer nanomaterials in detecting cTnI by electrochemical biosensors. We also discuss the application of various electrochemical biosensors in biomarker detection under different techniques. Moreover, this review systematically reveals its mechanism of action and unique benefits. It focuses on systematically presenting the latest research progress in the detection of cardiac biomarkers based on electrochemical platforms. We deeply analyze their current application status and future development trends, geared towards providing a comprehensive and future reference for research.

Received 26th June 2025
Accepted 14th July 2025

DOI: 10.1039/d5ra04555j

rsc.li/rsc-advances

1. Introduction

Cardiovascular disease (CVD) is a class of diseases of the heart and vascular system responsible for a major global health challenge.[1–13] The World Health Organization's (WHO) 2024 report indicates that CVD is the leading cause of death globally.[14–20] The occurrence and development of CVD result from various factors, such as hyperlipidemia, high blood pressure, smoking, mental stress, lack of exercise or limited activity, improper diet, air pollution, gender differences (with a relatively higher incidence in men), and family genetic history.[21–23] The prevalence of CVD is significantly increasing as the global aging population increases. Besides, CVD risk factors continue to pose a threat to human health.[24–27]

Clinically, AMI is a severe cardiovascular disease.[17,28–34] It occurs when a coronary artery is blocked, before the corresponding myocardial area becomes hypoxic due to lack of blood supply, causing a sudden interruption of blood circulation in part of the myocardium.[35–38] This in turn causes damage and necrosis of myocardial cells, leading to severe consequences including heart failure, arrhythmia, cardiogenic shock, and cardiac arrest. The common cardiac markers include cTnI, cardiac troponin T (cTnT), C-reactive protein (CRP), myoglobin, lipoprotein-associated phospholipase, interleukin-6 (IL-6), interleukin-1 (IL-1), myeloperoxidase (MPO), and tumor necrosis factor-α (TNF-α). Among them, cTnI has extremely high specificity and sensitivity for acute cardiomyocyte injury and are the preferred biomarker for diagnosing AMI, *i.e.*, the "gold standard" for diagnosis.

Various techniques for identifying and detecting cTnI have been developed, including electrochemical biosensors, which have become the most broadly used basic type due to their significant benefits including high detection accuracy, low manufacturing cost, easy miniaturization, and high sensitivity.[39–41] Unlike classical immunoassay techniques, electrochemical analysis methods have displayed several advantages and opened up new avenues for compound detection, with significant promise in the biomedical field.[42–44]

Electrochemical biosensors are moving towards refinement and diversification with the continuous advancement of technology. Common electrochemical determination methods include electrochemical immunosensors,[45–51] field-effect transistors (FETs),[52–56] electrochemical aptamers,[57–65]

[a]*Henan Institute of Technology School of Materials Science and Engineering, Xinxiang, 453003, China*
[b]*School of Chemistry and Chemical Engineering, Henan Institute of Science and Technology, Xinxiang, 453003, China*

electrochemiluminescence immunoassay (ECLIA),[66–75] and the cross-application of multiple techniques.[76–81] In the field of electrochemical bioassay, carbon-based materials, metal matrix composites, ceramic matrix composites, MOF composites, *etc.* presently act as sensor construction media. This provides a reference for developing electrochemical assay technology and strongly promotes progress in this field.

Carbon-based materials include graphene, carbon nanotubes, graphene quantum dots, *etc.* Graphene is two-dimensional honeycomb-like, with high electrical conductivity and electrocatalytic activity, large specific surface area, and good biocompatibility.[82–88] Carbon nanotubes are tubular nanomaterials with high-strength thermal conductivity and good modifiability. Graphene quantum dots have excellent optical and electrical properties as zero-dimensional nanomaterials. Nonetheless, single carbon-based materials are prone to agglomeration due to their high specific surface area and strong van der Waals forces. Besides, they are unevenly dispersed in the polymer matrix during conductive polymerization, hence reducing their conductivity.[89–92] Thus, other materials are often introduced to integrate with it to produce well-dispersed carbon-based composites. This provides a microenvironment appropriate for electrochemical reactions, as well as a large specific surface area and abundant active sites for effective identification and rapid detection of target substances.

Metal matrix composites have good electrical conductivity, which can shorten the distance between the electron donor and acceptor as well as improve the selectivity and sensitivity of the sensor. Among them, gold nanomaterials can improve electron transport, immobilize biomolecules, amplify signals, and improve stability and selectivity. They are also important materials for electrochemical biosensors. With their unique crystal structure and multi-metal synergistic properties, polymetallic super-structured nanocrystals can improve electron conduction, accelerate electrochemical reactions, and load numerous biometric molecules for signal amplification.[93–96]

Ceramic matrix composites, with inorganic ceramics including metal oxides as the main body and metal oxides such as CuO, ZnO, Fe_3O_4, TiO_2 and SiO_2 as the base, combined with carbon materials, polymers, or other nanomaterial particles are broadly used in catalysis, energy storage, and electrochemical sensing. This material has outstanding benefits including high chemical stability, good adsorption performance, adjustable electrical properties, and strong material compatibility, providing a strong impetus for developing electrochemical detection of cTnI.

Metal–organic framework (MOFs) composites comprising metal ions and organic ligands have high specific surface area and porosity, strong catalytic efficiency, and good stability.[97,98] They can be used to construct sensor electrodes and as signal amplification materials for highly sensitive detection of various substances including biomolecules. To improve their sensitivity and detection efficiency, composites including MOF/carbon, MOF/metal nanoparticles, MOF/metal oxides, and MOF/enzymes have emerged one after another, making it possible to identify excellent electrode materials for electrochemical biosensors.

In the current dispensation of biomedical detection technology, electrochemical biosensors are gradually emerging and showing great potential as a vital type of sensing device.[99,100] This review will systematically investigate the use of various electrochemical biosensing materials in sensor construction, comprehensively analyze their peculiar sensing mechanisms and detection benefits, as well as focus on the sensitivity performance of each material corresponding to the detection method.[101–106] We will also quantify their response capacity to small changes in the concentration of target cardiac biomarkers, which is important in key areas including early disease diagnosis.

Furthermore, we will closely integrate with biomedical clinical application scenarios to analyze the efficacy of these methods in actual medical settings.[107–110] Through systematic comparison, we will provide highly valuable references for researchers in material selection. This review will provide comprehensive and strong support for further development and improvement of biomarker detection technology based on electrochemical biosensors. The review will also promote wider and deeper use of this technology in the biomedical field.[111–114]

2. Carbon-based materials

Carbon materials, including graphene, carbon nanotubes, graphene quantum dots, *etc.*, which have good electrical conductivity, large specific surface area, and several functional groups have been used in supercapacitors, electrocatalysis, and batteries. Carbon-based materials with excellent dispersibility were successfully prepared by introducing nanoparticles to separate individual sheets. The composite materials formed have high porosity, large surface area, high catalytic efficiency, and good electrical conductivity, hence widely used in the research and development of electrochemical biosensors with high sensitivity and selectivity.

2.1 Graphene-based composites

As a typical two-dimensional carbon nanomaterial, graphene has a unique honeycomb-like lattice structure in which carbon atoms are closely linked in sp^2 hybridization to form a stable hexagonal network plane. This special structure endows graphene with excellent features including high electrical conductivity, good electrocatalytic activity, large specific surface area, and good biocompatibility. Because of these properties, graphene has been broadly used in electrochemical sensors and biosensors, demonstrating significant potential for use in disease marker detection.

Nitin K. Puri *et al.*[115] fabricated an electrochemical immunosensor based on hydrothermal synthesis of tungsten trioxide–reduced graphene oxide (WO_3–RGO) nanocomposites for detecting cardiac biomarker cTnI (Fig. 1a). APTES/WO_3–RGO nanocomposite ITO films were obtained *via* electrophoretic deposition, before covalently fixing cTnI antibodies. The antibody molecules were strongly covalently coupled with the

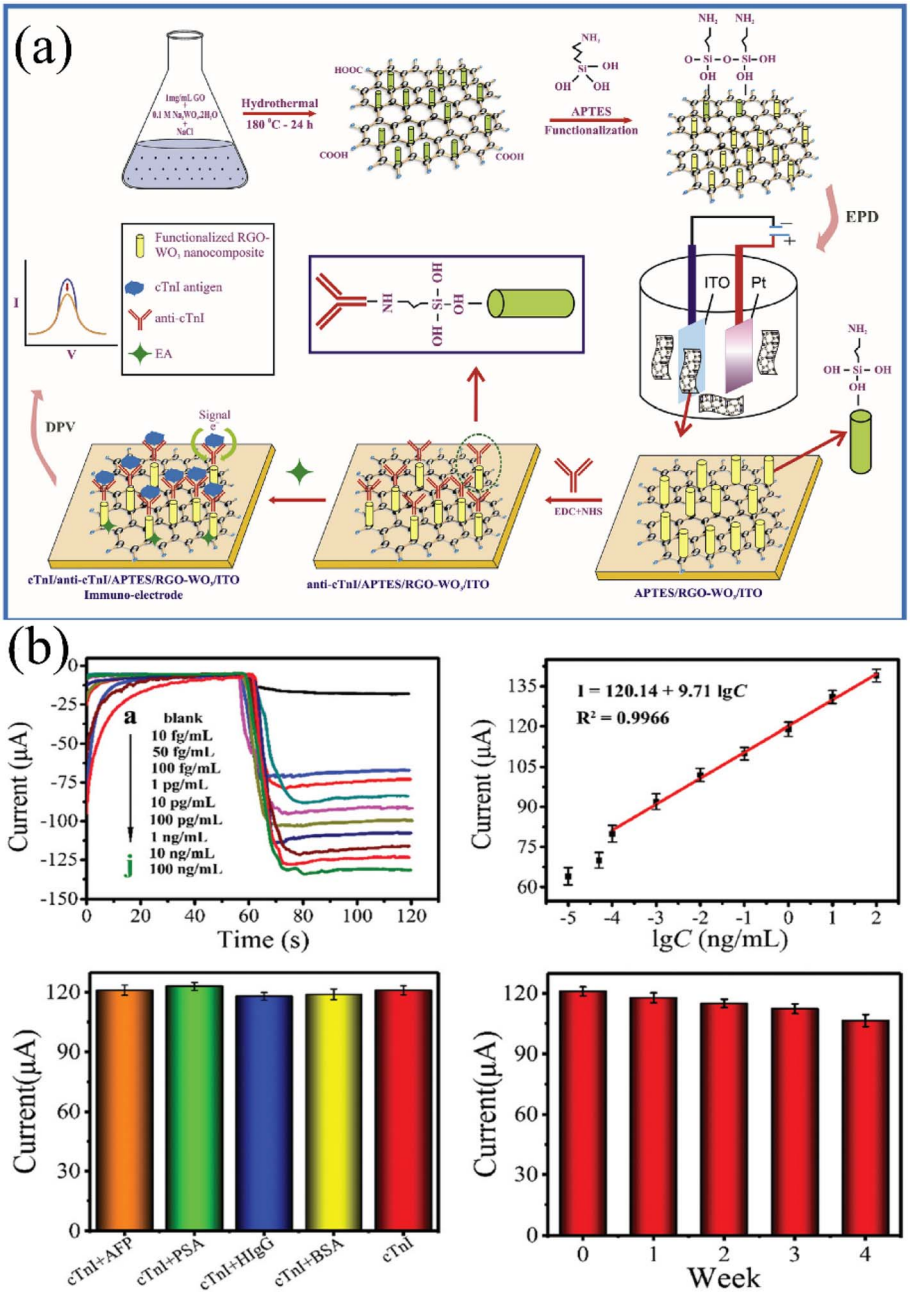

Fig. 1 (a) Schematic diagram of preparation process of the cTnI/APTES/WOs–RGO nanocomposite/ITO immunosensor and its molecular recognition of cTnI; reproduced from ref. 115 with permission from Elsevier, copyright 2018. (b) Schematic diagram of amperometric *i*–*t* responses of the CDs-3D-PG-Pd@Au nanoclusters-modified immunosensor upon incubation with various concentrations of cTnI and its selectivity and stability evaluation of the immunosensor. Reproduced from ref. 116 with permission from Royal Society of Chemistry, copyright 2019.

WO_3–RGO nanocomposite matrix through APTES, offering the device high stability. The study revealed that the immunosensor of the WO_3–RGO nanocomposites performed well, with high sensitivity in the detection range of 0.01–250 ng mL^{-1}.

To further break through the performance limitations of single-material systems, Yueyun Li *et al.*[116] developed an electrochemical immunosensor based on the effective signal amplification strategy of CDs-3D-PG-Pd@Au NCs electrocatalysis and thionine (Th)-mediated H_2O_2 reduction. Notably, β-cyclodextrin (CDs) has two important roles, which can improve the dispersion of three-dimensional porous graphene (3D-PG) and show good capture capacity for secondary antibodies (Ab_2) (Fig. 1b). Under optimal conditions, immunosensors based on these materials demonstrated high selectivity and good reproducibility for cTnI detection, with a low detection limit (LOD) of 33.3 fg mL^{-1}. This provides an effective strategy for clinical research with their special material combination.

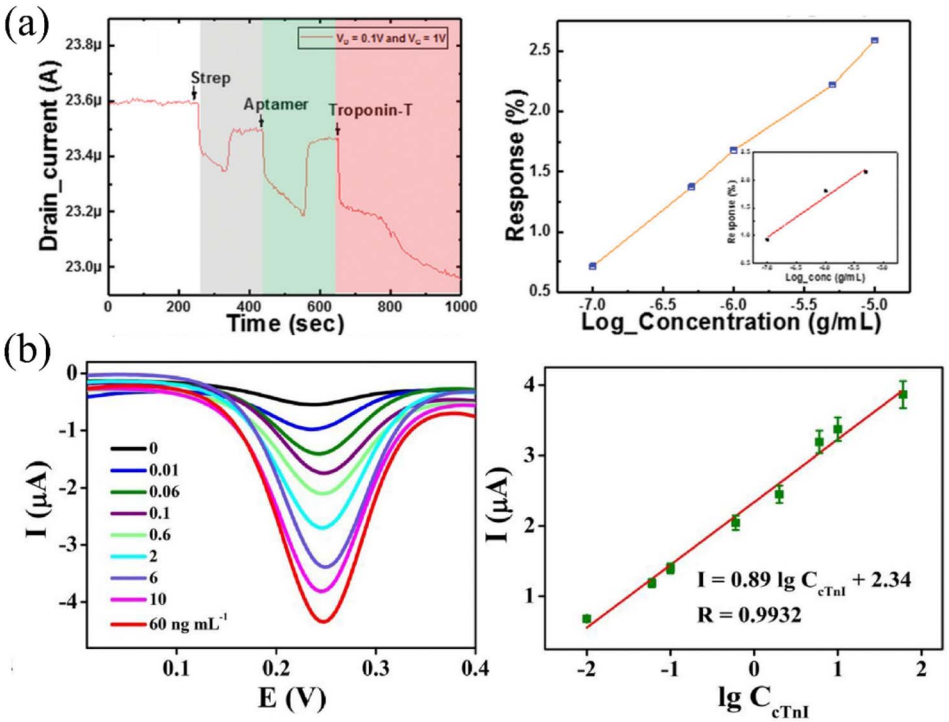

Fig. 2 (a) Transient response (drain current) of the device with low concentration and the response of the devices for different concentrations of analyte to identify the LOD. The inset shows the linearity curve; reproduced from ref. 118 with permission from Royal Society of Chemistry, copyright 2020. (b) DPV curves of the Ab-Fc-COOH/cTnI/BSA/anti-cTnI/CIL–HCNTs/GCE immunosensor after incubation with various concentrations of cTnI from 0 to 60 ng per mL cTnI, and calibration curves of the immunosensor to different concentrations of cTnI. Reproduced from ref. 120 with permission from Elsevier, copyright 2018.

2.2 Carbon nanotube-based composites

As a tubular nanomaterial made up of carbon atoms, carbon nanotubes have a unique structure and several significant benefits. The material has extremely high strength and thermal conductivity, excellent flexibility, and good electrical conductivity, making it possible to miniaturize electronic devices. Moreover, carbon nanotubes have good modifiability. Specific recognition of particular substances can be achieved by introducing functional groups or biomolecules, greatly expanding the application range. Synergistic effects can be produced to further optimize sensor performance when combined with other materials, thus enabling the construction of high-performance sensors for detecting biomolecules and chemicals.

Taek Lee *et al.*[117] constructed a fast electrochemical biosensor based on a carbon nanotube network (CNN) on a microelectrode array and DNA aptamers, which can detect cTnI in human serum samples within 10 minutes. They introduced an alternating current electrothermal flow (ACEF) method to improve the affinity between DNA aptamers and target molecules. The biosensor detects cTnI in a range of 1 pM to 100 nM with a LOD of 6.59 fM, which is expected to promote rapid early detection of AMI in the future.

To address the limitation of DNA aptamers' long-term application potential due to their biological stability issues, Sandeep G. Surya *et al.*[118] developed a universal and stable single-walled carbon nanotube field-effect transistor (SWCNT FET) sensor using a synergistic combination of precious metal nanoparticles (AuNPs) and Co_3O_4, with a synergistic effect of Co_3O_4 nanorods and gold nanoparticles (Fig. 2a). The developed device could detect cTnI with a sensitivity of up to 0.5 mA mg^{-1} mL^{-1} and a LOD of 0.1 mg mL^{-1}.

To further promote the clinical translation of the technology, Shreyas Vasantham *et al.*[119] constructed a paper-based sensing platform that combined carboxyl-functionalized multi-walled carbon nanotubes with anti-cardiac troponin I (cTnI) and characterized the properties using electrochemical impedance spectroscopy. The suitability of the immunosensor was verified by adding cTnI to serum samples. The sensor had a detection limit of 0.05 ng mL^{-1}, a sensitivity of 1.85 mΩ ng^{-1} mL^{-1}, a response of about 1 minute, and a shelf life of nearly 30 days. Impedance-type immunosensors were successfully developed based on a paper microfluidic analysis device and multi-walled carbon nanotubes. The sensor is economically viable with many benefits, hence providing support for early prediction of acute myocardial infarction.

Based on the existing technical foundation, Yanbo Zeng *et al.*[120] used the ultrasonic method to prepare carboxyl-terminated ionic liquid and helical carbon nanotube composites (CIL–HCNTs) (Fig. 2b). CIL–HCNTs provide a good platform for the fixation of anti-cTnI monoclonal antibodies through its carboxyl group due to the large specific surface area and high electrical conductivity of the composite. The signal marker Fc-COOH based on the oxidation process was combined with the

CIL–HCNTs platform to develop an electrochemical immunosensor for detecting cTnI, which showed excellent specificity and high reproducibility for analyzing human serum samples.

2.3 Graphene quantum dot composites

Graphene quantum dots (GQDs) are a class of zero-dimensional nanomaterials comprising carbon atoms, typically ranging in size from a few nanometers to tens of nanometers. Based on unique quantum confinement and edge effects, GQDs possess profound electrical properties with high carrier mobility and excellent optical properties including tunable fluorescence and wide absorption spectra, as well as good biocompatibility and low toxicity. This enables highly sensitive detection of multiple substances in sensor and biomedical fields.

Jiangnan Shu *et al.*[121] synthesized nanoluminescent *N*-(4-aminobutyl)-*n*-ethylimino-functionalized graphene quantum dots (ABEI@GQDs). In an aqueous solution, the luminescent material exhibited three completely potential-distinguishable bicolor ECL emissions upon reacting with co-reactant $K_2S_2O_8$. A label-free tripotential-ratio ECL immunosensor for detecting cTnI was developed by layer-by-layer assembly of ABEI@GQDs and antibodies on a chitosan-modified fluorine-doped tin oxide electrode. The linear range was 1.0 fg mL^{-1}–5.0 pg mL^{-1} with the LOD of 0.35 fg mL^{-1} when used to detect cTnI, outperforming the most reported ECL methods.

To address the specificity bottleneck of label-free systems, Yola *et al.*[122] developed a highly sensitive and selective sandwich electrochemical cTnI immunosensor using nitrogen–boron doped graphene quantum dots (N–B-GQDs) as electrode platforms and two-dimensional cerium-doped SnO_2/SnS_2 (Ce-SnO_2/SnS_2) as signal amplification materials (Fig. 3a). According to the EDX analysis in Fig. 3a, the elements O, S, Sn, and Ce were clearly detected in the Ce-SnO_2/SnS_2 heterojunction material, confirming the successful doping of Ce. Comparative spectral data show that the UV-Vis absorption bands of SnO_2 and SnS_2 are significantly weaker than those of the Ce-SnO_2/SnS_2 system, a phenomenon that directly indicates Ce doping effectively enhances the material's light absorption performance. This enhanced absorption capacity further strengthens the material's molecular recognition efficiency for cTnI (cardiac troponin I), providing strong support for its application in the field of biosensing. In preparation, anti-cTnI-Ab_1 was fixed to N–B-GQDs by coordination covalent bond; anti-cTnI-Ab_2 was bound to thiol-acetic acid-modified Ce-SnO_2/SnS_2 by esterification reaction. The sensor detected cTnI in plasma *via* antigen–antibody interaction, with a LOD of 2.00 fg mL^{-1}, and an effective tool detecting AMI.

Building on the solution for ECL applications in complex environments, Yueyun Li *et al.*[123] constructed a novel ECL biosensor using Co_3O_4 nanoarrays (NAs) as the sensing substrate and GQDs-coupled gold nanoclusters (AuNCs) nanocomposites as signal markers (Fig. 3b). After coupling with GQDs, the resulting quantum-state composites (AuNCs-GQDs) were spatially closely correlated, causing a stronger ECL response thanks to resonant energy transfer and synergistic effects. When the biosensor was used to detect cTnI, the linear range was 500 fg mL^{-1}–20 ng mL^{-1} with a low LOD of 354.2 fg mL^{-1}.

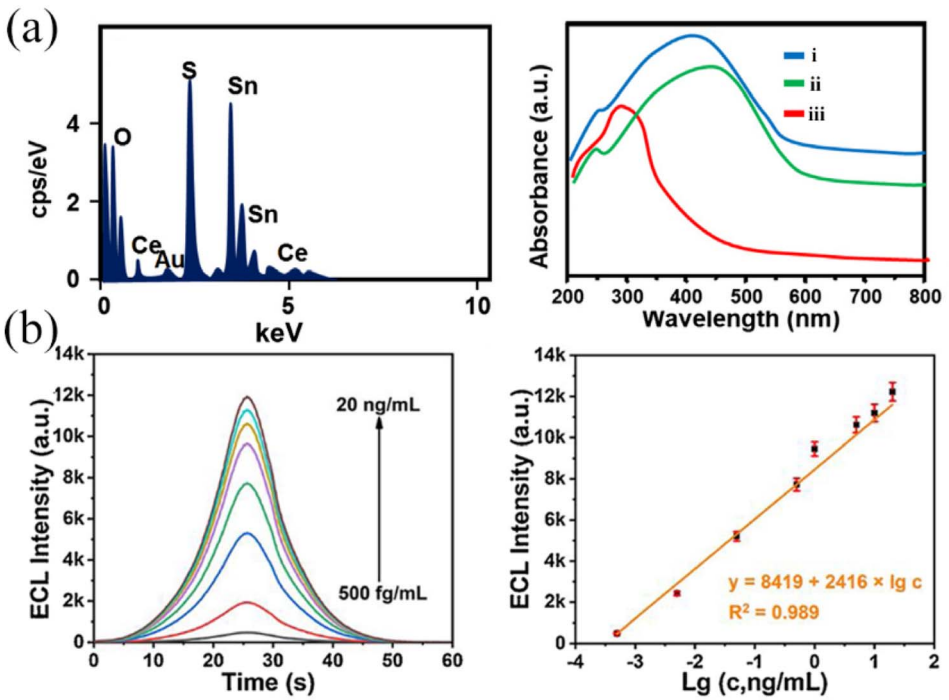

Fig. 3 (a) EDX image and UV-Vis spectra of Ce-SnO_2/SnS_2 (spectrum i), SnS_2 (spectrum ii) and SnO_2 (spectrum iii); reproduced from ref. 122 with permission from Elsevier, copyright 2022. (b) ECL intensity–times curves and calibration curve of the NH_2–Co_3O_4-Ab_1-BSA-cTnI-Au NCs-GQDs-Ab_2/GCE biosensor recognition of different concentrations of cTnI (ranging from 500 fg mL^{-1} to 20 ng mL^{-1}); reproduced from ref. 123 with permission from Elsevier, copyright 2021.

3. Metal matrix composites

Metal matrix composites, with metals or metal nanoparticles as the core components have attracted much attention because of their unique microstructure and excellent performance. These materials have good electrical conductivity, and significantly shorten the distance between the electron donor and acceptor, thereby effectively accelerating electron transfer to the electrode surface. Due to this property, metal matrix composites can significantly improve the selectivity and sensitivity of corresponding response sensors in their applications, enabling accurate capture and identification of specific substances. Consequently, metal matrix composites are extensively used in frontier fields including catalysis, sensing, and biomedicine, thus providing important support for technological innovation and development in various industries.

3.1 Gold nanocomposites

Gold nanomaterials are indispensable key materials in the field of electrochemical immunosensors because of their significant roles in improving electron transport, biomolecular immobilization, signal amplification, stability, and selectivity, as well as synergies with other materials. Additionally, developing new electrochemical biosensors based on cardiac troponin by integrating gold nanoparticles with other different materials as new composite materials as support materials provides a strong impetus for advancing the field of cTnI detection.

Di Yang *et al.*[124] prepared hydroxyl-rich carbon quantum dots to help in synthesizing gold nanoparticles (C-dots@AuNP). They also constructed a sandwich immunosensor on a chitosan-modified glassy carbon electrode (GCE) through glutaraldehyde (GA) cross-linking. Carbon dots (C-dots) and C-dots@AuNP catalyzed the reaction between Cu^{2+} and ascorbic acid (AA) to form copper nanoparticles (CuNPs) and coat the nanoparticles, thereby amplifying the detection signal (Fig. 4a). The electrodes prepared using anodic stripping square wave voltammetry (ASSWV) reduced the LOD of cTnI to the fg mL^{-1} level.

However, this amplification strategy based on electrode surface modification is prone to matrix interference in complex biological samples. To address this issue, S. C. B. Gopinath *et al.*[125] developed interdigital electrode sensors with different surface interfaces for detecting cardiac biomarker cTnI using capture aptamer-conjugated gold nanoparticle probes and detection antibody probes and comparing them with alternating sandwich modes (Fig. 4b). They found that the LOD of cTnI was 1 fM when using antibody and 100 aM when using aptamer-gold-cTnI-antibody sandwich mode. The sensor also demonstrated higher specificity and excellent anti-contamination capacity.

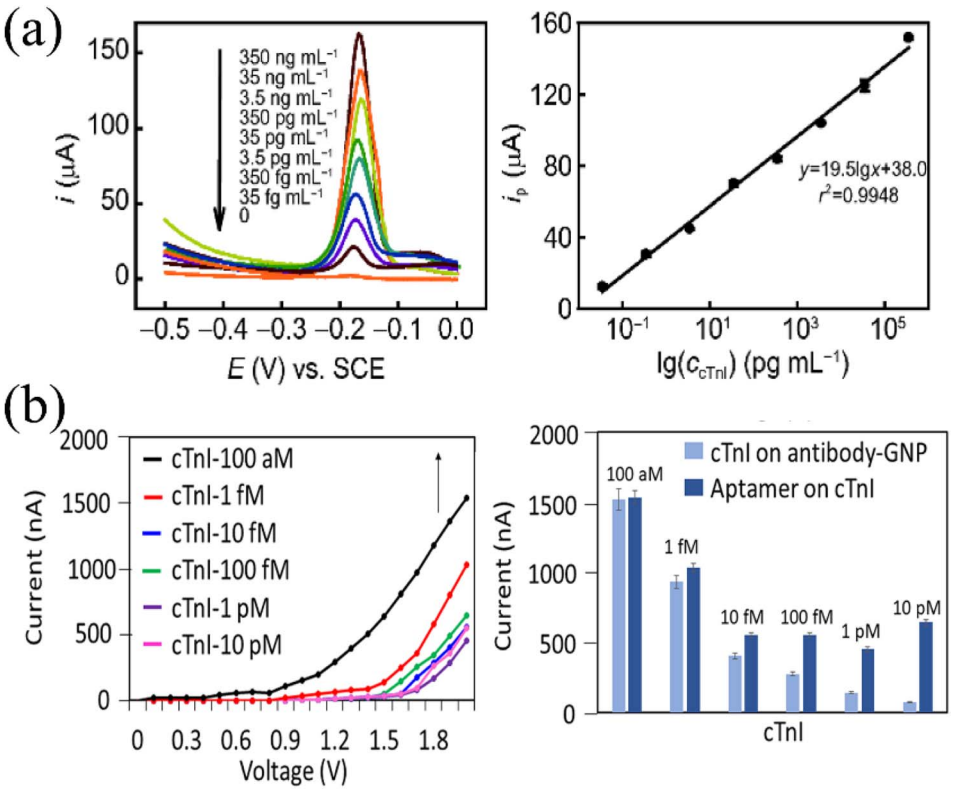

Fig. 4 (a) The ASSWV curves for cTnI and IgG immunoassay and standard curves. Reproduced from ref. 124 with permission from Wiley, copyright 2018. (b) Immunosensor based on antibody-cTnI-aptamer sandwich architecture for detection of cTnI (100 aM to 10 pM) and schematic comparison of current changes induced by cTnI interactions with antibody and aptamer; reproduced from ref. 125 with permission from Springer, copyright 2022.

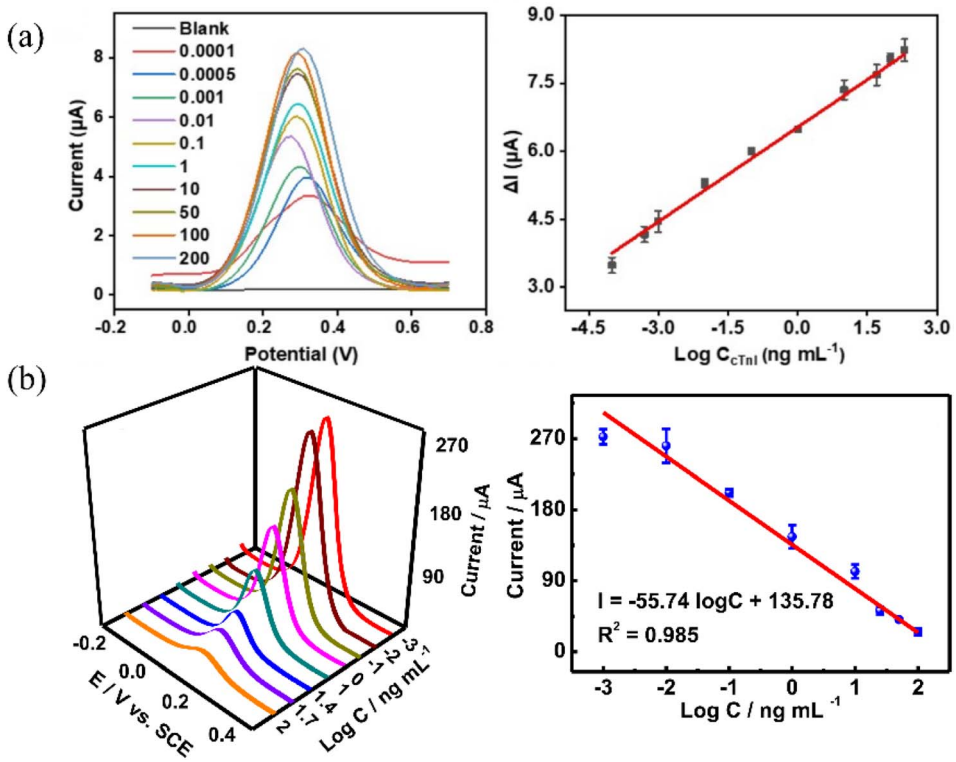

Fig. 5 (a) Schematic diagram of the Pd@PdPtCo MNPs biosensor for cTnI detection (concentration from 0.0001 to 200 ng mL^{-1}) and linear calibration curve of ΔI *vs.* Log C_{cTnI} for the immunosensor; reproduced from ref. 127 with permission from Elsevier, copyright 2025. (b) Electrochemical immunosensor based on PtCoCuPd hexagonal bipyramidal tetrametallic nanoparticles (HBTPs) for detection of cTnI at different concentrations (0.001–100.0 ng mL^{-1}) and schematic diagrams of DPV and calibration curves. Reproduced from ref. 128 with permission from Elsevier, copyright 2019.

To simplify the detection process and explore new sensing mechanisms, Vijayender Bhalla *et al.*[62] fabricated a label-free electrochemical aptamer sensor by self-assembling aptamer-coupled gold nanoparticles (GNP-A) and uniformly arranging them on GO sheets to produce GO@GNP-A nanohybrids, before modifying them with biomarkers. Detection by redox active molecules revealed that the interaction between cTnI and nanohybrids at the aptamer biological interface enhanced the electrochemical signal. Since cTnI binding causes conformational changes and charge neutralization of the aptamer, which causes a continuous increase in the current signal, the sensor can identify cTnI with a sensitivity of 0.001 pg mL^{-1}; this enables highly sensitive and efficient quick detection.

To integrate wide-range detection with ultra-sensitive characteristics, Xiurong Yang *et al.*[126] developed an ultra-sensitive ECL immunosensor for identifying cTnI using gold nanocluster (Au NCs) and hybridization chain reaction (HCR) signal amplification techniques. They double-labeled AuNCs at both ends of hairpin DNA (H_1 and H_2) as light emitters, and attached the DNA initiation strand (T_1) and secondary antibody (Ab_2) to gold nanoparticles (AuNPs) to create intelligent probes (Ab_2–AuNP–T_1). The sensor detected cTnI at a range of 5 fg mL^{-1} to 50 ng mL^{-1} with a low LOD of 1.01 fg mL^{-1}.

3.2 Polymetallic super-structured nanocrystals

Polymetallic superstructured nanocrystals play a key role in electrochemical immunosensors. These materials have demonstrated excellent performance due to their peculiar crystal structure and multi-metal synergies. On one hand, its special structure can effectively improve electron conduction, significantly accelerate electrochemical reaction rates, and improve the timeliness of sensing responses. On the other hand, the combination of multiple metals endows it with a strong loading capacity, which can fix several biometric molecules and achieve efficient amplification of the signal. As a consequence, it improves the sensitivity and accuracy of the detection, hence providing important support for developing electrochemical immunosensor technology.

Qing Liu *et al.*[48] fabricated a highly conductive polypyrrole (PPy) functionalized dice-shaped cobalt square cage (DCSC) and loaded polyhedral spherical PdCuPt nanoparticles (NPs) onto it to develop an unlabeled electrochemical immunosensor for ultra-sensitive detection of cTnI. Due to its excellent performance of PdCuPt/PPY/DCSC nanocomposites as an electrical signal amplification platform, the constructed immunosensor has high sensitivity, low LOD (16.03 fg mL^{-1}), wide detection range (50 fg mL^{-1}–1 μg mL^{-1}), good reproducibility, selectivity, and stability.

However, the signal amplification efficiency of this system is still limited by the uniform dispersion of nanoparticles on the

carrier surface. To resolve the problem, Shan-Shan Li *et al.*[127] synthesized mesoporous nanopolyhedra (MNPs) with large specific surface area and multiple active sites, which were used as signal amplifiers to design a sensitive electrochemical biosensor for cTnI analysis (Fig. 5a). Under the optimized conditions, the prepared biosensor had a wide linear range (1.0×10^{-4}–200 ng mL^{-1}) and a low LOD (0.031 pg mL^{-1}), along with good stability and high sensitivity.

To further break through the interfacial catalysis bottleneck of multimetallic systems, Jiu-Ju Feng *et al.*[128] synthesized a four-metal PtCoCuPd hierarchical branched tripod structure (HBTPs) before using it to construct a novel label-free immunosensor for detecting cTnI (Fig. 5b). The unique hierarchical micro–nano structure significantly improved the immobilization of antibodies and enhanced the catalytic activity for potassium ferricyanide ($K_3Fe(CN)_6$), effectively amplifying the electrochemical signal and improving the detection sensitivity. Under the optimal conditions, the prepared immunosensor displayed a wide linear range (0.001–100.0 ng mL^{-1}) and a low LOD (0.2 pg mL^{-1}) for cTnI detection.

4. Ceramic matrix composites

Ceramic matrix composites (CuO, ZnO, Fe_3O_4, TiO_2, SiO_2, *etc.*) have a large specific surface area and abundant active sites, which can provide an appropriate microenvironment for the electrochemical reaction of the target molecule. This promotes effective identification and rapid detection of the target substance, a new type of electrochemical biosensor based on cTnI. It provides a strong impetus for developing electrochemical detection of cTnI.

Yueyun Li *et al.*[69] prepared a composite material of glutathione–gold nanoclusters coated on reduced graphene oxide (GSH–Au NCs@rGO) and gold nanoparticles functionalized copper oxide (Au@CuO), and constructed a "signal-off" ECL biosensing platform. As an ECL luminophore, GSH–Au NCs@rGO can not only load more luminescent groups and immobilize biological receptor units, but also accelerate ECL excitation by promoting mass transfer, significantly enhancing the luminescence signal intensity. Au@CuO with good biocompatibility is used as a quenching probe, and the RET between acceptor and GSH–Au NCs@rGO (donor) can

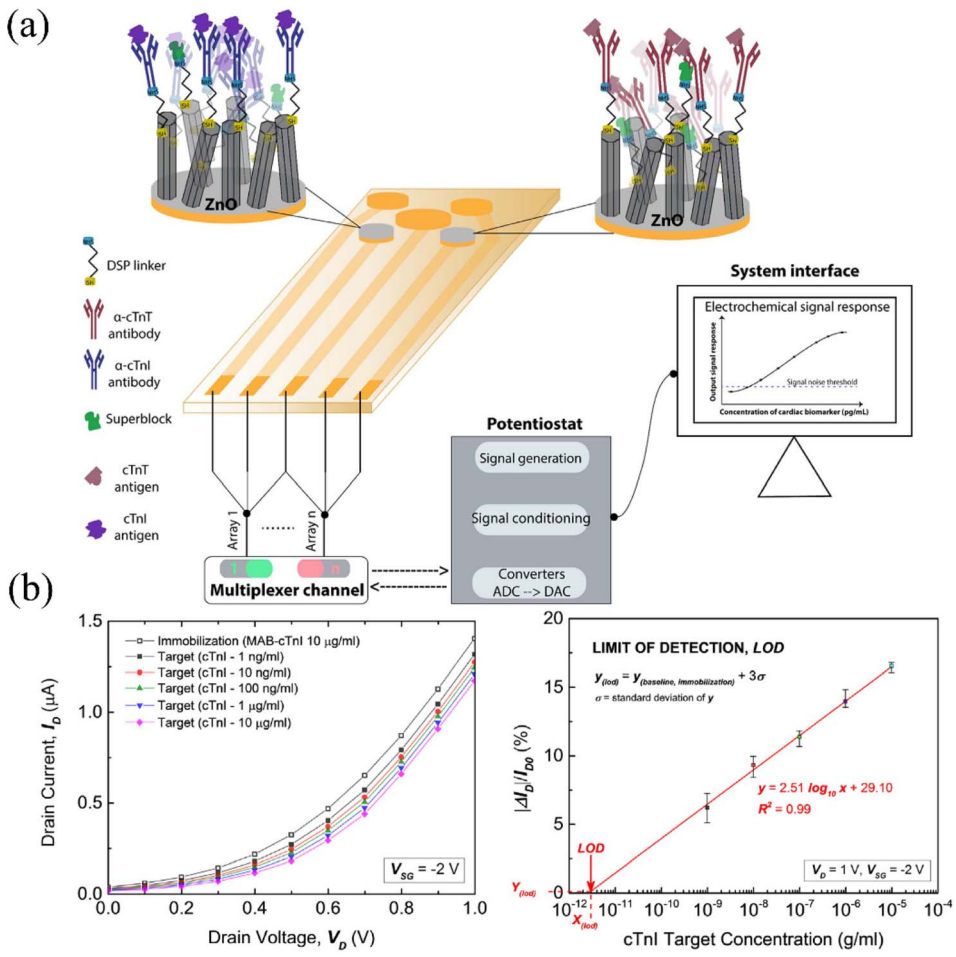

Fig. 6 (a) Schematic representation of sensing of cTnI and cTnT biomarkers in multiplexed sensor array format; reproduced from ref. 129 with permission from Elsevier, copyright 2017. (b) Detection of cTnI target biomarker at different concentrations (1 ng mL^{-1} to 10 μg mL^{-1}) using the ZnO-FET biosensor, and calibration curves of immunosensor to different concentrations of cTnI. Reproduced from ref. 130 with permission from Elsevier, copyright 2017.

effectively quench the ECL intensity to a reasonable range required for trace analysis. Evaluation with cTnI as a model analyte shows that the platform has a low detection limit of 54.95 fg mL^{-1}, providing a new strategy for the sensitive detection of biomarkers in early clinical diagnosis of diseases.

However, the ultrasensitive detection of a single biomarker is difficult to meet the needs of clinical multi-marker combined diagnosis. To address this challenge, Sriram Muthukumar *et al.*[129] developed flexible disposable electrochemical biosensors based on vertically oriented zinc oxide nanostructures for rapid simultaneous screening of cTnI and cTnT. By fabricating electrodes by growing ZnO nanostructures on working electrodes and using nanostructures to limit target molecules for multiple detections, cTnI and cTnT in human serum were limited to 1 pg mL^{-1} (Fig. 6a). This is the first platform to achieve simultaneous multiplex detection using multiple configurable methods. The strategy based on affinity sensing is anticipated to be applied to other biomarker detection with clinical translational prospects.

Meanwhile, in the field of integration of nanomaterials and semiconductor devices, K. Md. Arshad *et al.*[130] took device architecture innovation as the breakthrough point, and achieved dual breakthroughs in detection sensitivity and signal transduction efficiency through the integration of FET technology and ZnO nanofilms. They found that zinc oxide nanoparticles (ZnO-NPs) thin film materials were deposited on the channel by sol–gel and spin-coating techniques. The LOD for detecting cTnI was as low as 3.24 pg mL^{-1} (Fig. 6b), and the sensitivity of both methods was greatly improved, opening up new avenues for future development of new FET biosensors using advanced nanomaterials.

Soo Suk Lee *et al.*[131] developed a highly sensitive and reproducible quartz crystal microbalance (QCM) immunosensor for detecting cTnI in human serum. The method employs a pair of

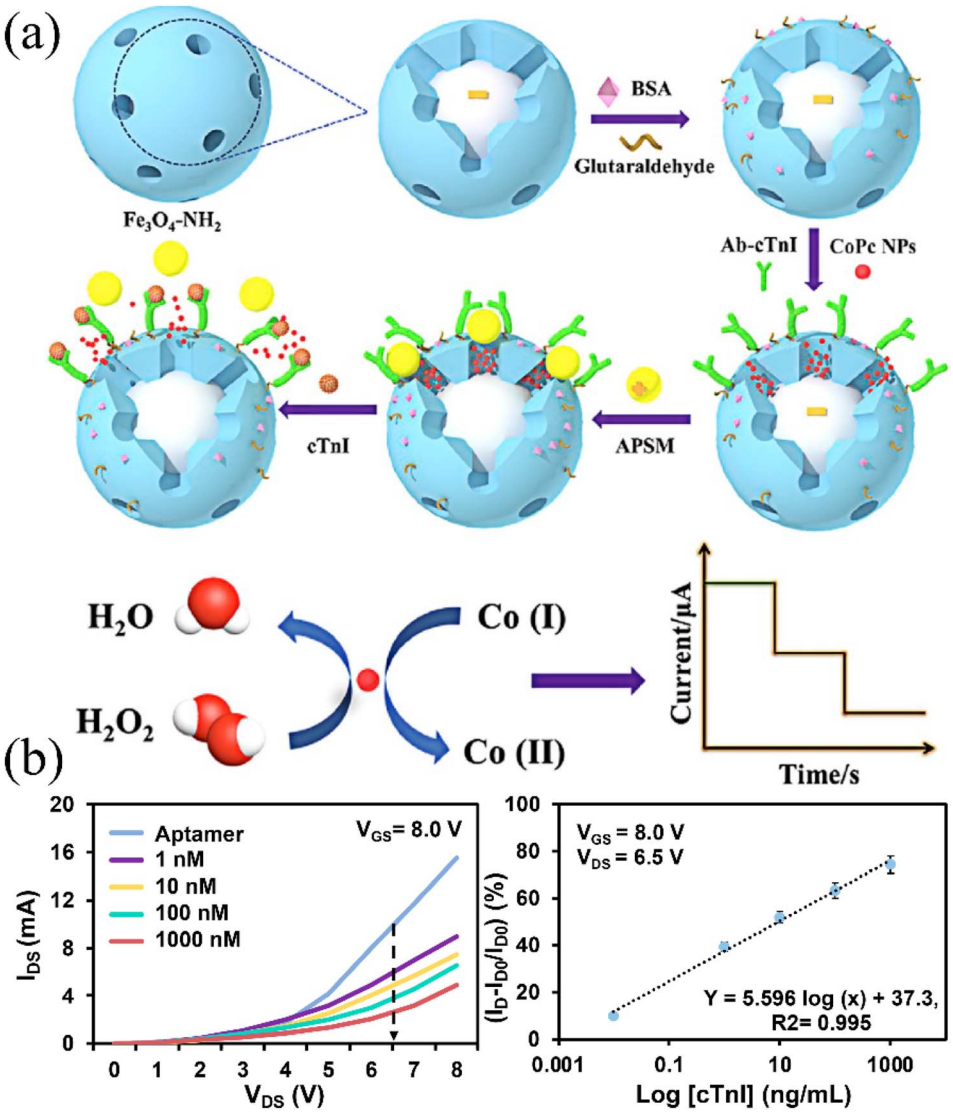

Fig. 7 (a) The preparation process of the APSM-capped CoPc NPs Fe_3O_4-Ab/MGCE sandwich electrochemical immunosensor; reproduced from ref. 133 with permission from Elsevier, copyright 2019. (b) Molecular recognition of cTnI at concentrations from 1.0 ng mL^{-1} to 1.0 μg mL^{-1} using an Au/PCN-FET biosensor and corresponding calibration curve. Reproduced from ref. 134 with permission from MDPI, copyright 2022.

capture antibodies binding to different epitopes of cTnI to construct a sandwich immunoassay system, while using photocatalytic silver staining to amplify the size of TiO_2 nanoparticles for signal enhancement. QCM enables quantitative analysis by monitoring resonance frequency shifts caused by mass changes on the sensor surface. Results show that the detection limit of cTnI decreases from 307 pg mL^{-1} to 18 pg mL^{-1} after signal amplification, significantly improving the sensitivity and reproducibility of cTnI detection in human serum.

However, the clinical diagnosis of AMI often requires comprehensive evaluation of multiple biomarkers, and the detection of a single indicator has limitations. Xin Rui Wang *et al.*[132] constructed hierarchical magnetic core/multishell lanthanide metal–organic framework (Ln-MOF) nanospheres Fe_2O_3@SiO_2@Eu-MOF@Tb-MOF (MagMOF) *via* a layer-by-layer self-assembly (LBL) strategy. By further conjugating target mRNA sequences and specific antibodies (NH_2-mRNA, anti-cTnI, and anti-Mb antibodies), a mixed sensing platform was developed for highly sensitive detection of CK-MB, Mb, and cTnI, with detection limits of 174.98 U L^{-1}, 0.16 mg L^{-1}, and 0.94 mg L^{-1}, respectively. The detection ranges of MagMOF for the above indices in human serum cover the clinical normal ranges. This represents the first example of stable, sensitive, rapid, and convenient detection of these AMI biomarkers and the therapeutic drug aspirin.

In the field of high-sensitivity detection for single biomarkers, Dan Wu *et al.*[133] took the functional design of nanocontainers as a breakthrough, achieving an order-of-magnitude improvement in detection accuracy through a molecular gating strategy. They used aminated polystyrene microspheres (APSM) as molecular gates and iron(III) oxide (Fe_3O_4) as nano-containers. Amino-functionalized mesoporous ferric oxide (Fe_3O_4–NH_2) was used to load cobalt

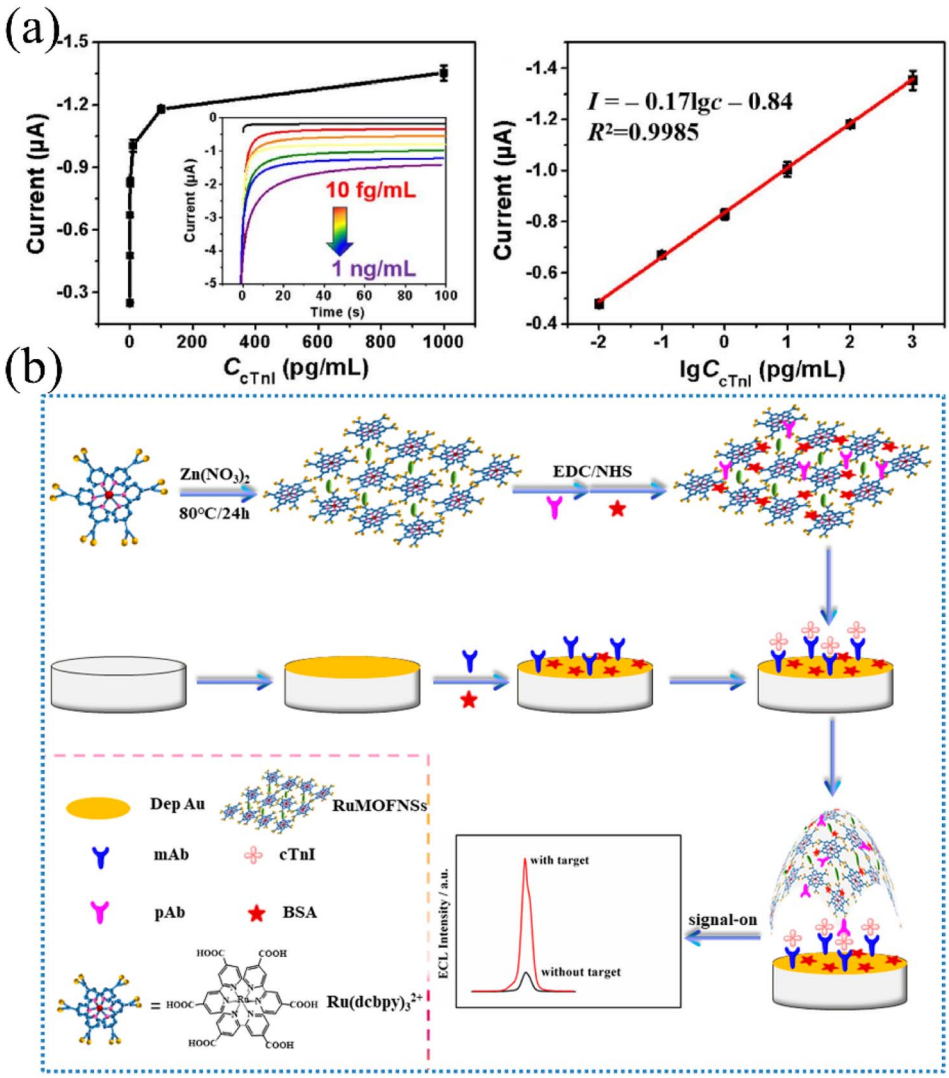

Fig. 8 (a) Schematic diagram of high-sensitivity current response of ZIF-67@PBA dual-aptamer sensor to cTnI and calibration curve between current intensity and logarithm of cTnI concentration in the range of 10 fg mL^{-1} to 1 ng mL^{-1}; reproduced from ref. 135 with permission from Elsevier, copyright 2025. (b) Schematic diagram of RuMOFNSs-Ab_1/cTnI/BSA/mAb/depAu/GCE ECL immunosensor fabrication process. Reproduced from ref. 136 with permission from Analytical Chemistry, copyright 2019.

phthalocyanine nanoparticles (CoPc NPs) and further capture antibodies (Ab) of cTnI to form Fe_3O_4-Ab. The sensor has a wide linear range from 1.0 pg mL^{-1} to 100 ng mL^{-1} with a low LOD of 0.39 pg mL^{-1} under optimal conditions (Fig. 7a). The immunosensor also has good reproducibility and selectivity, giving it broad application prospects in clinical studies.

With the development of biosensing technology towards integration and device-oriented directions, Nabil Salama *et al.* by using indium gallium zinc oxide (IGZO) as an excellent semiconductor channel and combining it with nanosheet materials, successfully applied it to FET biosensing technology with a detection range of 0.01–1000 ng mL^{-1}. The detection limit was 0.0066 ng mL^{-1} (Fig. 7b).[134] In this sensing technique, gold nanoparticle (AuNPs)-modified porous carbon nitride (PCN) is used as a bridge between solid-state devices and cTnI, which has a porous structure as well as a large surface area and is more conducive to aptamer fixation. This provides a strong reference for enhancing the combination of cTnI and transistors to detect other biomolecules.

5. Metal–organic framework (MOFs) composites

Studies have shown have that MOFs composites play a significant role in material science due to their unique structural and performance advantages. They have a rich and regular pore structure, combined with an extremely high specific surface area that provides ample space for storage and reaction of substances. Good electrical conductivity and chemical stability ensure stable operation of the material in various environments. Numerous active sites endow it with multifunctional properties, simultaneously enabling adsorption, catalysis, sensing, and other functions. Consequently, MOFs composites are broadly used in frontier fields including electrocatalytic synthesis and electrochemical biosensors.

Yun-Ming Wang *et al.*[45] developed a well-performing MOF-based nickel foam (NF)-loaded three-dimensional (3D) immunosensor (Ab-NH_2-MIL-88B-(Fe_2Co)-MOF/NF) for specific detection of cTnI. The electrochemical impedance spectroscopy (EIS) method was used to perform the electrochemical study by monitoring changes in charge transfer resistance (R_{ct}) characteristics. The LOD of the Ab-NH_2-MIL-88B (Fe_2Co)-MOF/NF immunosensor was as low as 13 fg mL^{-1}.

On the basis of three-dimensional structural sensing systems, researchers have further explored the optimization path of material interface design for detection performance. Yazhen Wang *et al.*[135] prepared zeolite imidazoline-skeleton structure-67 (ZIF-67) material with a high specific surface area by hydrothermal synthesis before *in situ* growth Prussian blue analogues (PBA) on its surface through ion exchange to generate MOF-on-MOF heterostructure (ZIF-67@PBA) material. Nitrogen-doped derived electrocatalyst N-ZIF-67@PBA was obtained by low-temperature calcination (Fig. 8a). The electrocatalyst was utilized as a signal amplifier and integrated with the efficient separation effect of magnetic beads to develop a magnetic dual aptamer electrochemical sensor for detecting cTnI. The LOD was as low as 0.31 fg mL^{-1}, confirming the potential of MOF materials in electrochemical aptamer sensing.

In terms of dimensional design and functional expansion of MOF materials, Xiurong Yang *et al.*[136] synthesized 2-D MOF nanosheets (RuMOFNSs) with excellent ECL properties using carboxyl tris(4,4′-dicarboxylic acid-2,2′-bipyridyl)ruthenium(II) ($Ru(dcbpy)_3^{2+}$) as organic ligands in a one-pot method as ECL luminescent bodies. A "signal-on" type ECL immunosensor for detecting cTnI was developed using this material as a probe (Fig. 8b). The immunosensor has high sensitivity and selectivity for detecting cTnI in the range of 1 fg mL^{-1} to 10 ng mL^{-1}, with a low LOD of 0.48 fg mL^{-1}.

On the basis of the single-component system of two-dimensional MOF nanosheets, researchers have further explored the ECL sensing strategy with synergistic enhancement of multi-materials. Ruo Yuan *et al.*[137] synthesized amino-functionalized metal–organic framework-modified carbon nitride nanosheets (CNNS@NH_2-MIL(Fe)) as an efficient ECL luminescent nanomaterial and constructed an ultra-sensitive ECL sensor for cTnI detection using Ti_3C_2 nanosheets as an excellent substrate. The LOD was as low as 0.38 fg mL^{-1}. The synthesized CNNS@NH_2-MIL(Fe) enabled CNNS payload, and accelerated reduction of co-reactant $S_2O_8^{2-}$ as well as enhanced the ECL signaling of CNNS.

6. Conductive polymer nanomaterials

Conductive polymers have been widely applied in cTnI detection due to their outstanding advantages, including high electrochemical activity, excellent electrical conductivity, strong surface modifiability, good biocompatibility, and simple preparation processes. Their unique nanostructures can effectively increase the specific surface area of materials, while composite materials can optimize the electron transport pathways. These two characteristics demonstrate remarkable potential in improving detection sensitivity and response speed.

Juankun Zhang *et al.*[138] constructed a novel molecularly imprinted polymer (MIP) sensor for rapid cTnI detection. The sensor specifically binds to cTnI, enabling serum cTnI concentration determination without complex pretreatment, with electrochemical signals correlated to template molecule concentration. It features simplicity, high specificity, low preparation cost, excellent chemical and mechanical properties, and sensitive label-free detection. The sensor exhibits good linearity in the 0.05–5.00 nM range, a detection limit of 0.027 nM, and a total detection time within 5 minutes.

Building on the foundation of rapid detection technologies, researchers have further explored integrated sensing solutions that combine high sensitivity with portability. Changill Ban *et al.*[139] constructed a sandwich aptamer-based screen-printed carbon electrode (SPCE) for chronoamperometric detection of cTnI. The disposable three-electrode SPCE was modified by electrodeposition of gold nanoparticles and electropolymerization of conductive polymers, enabling cTnI quantification *via* amperometric signals from the catalytic reaction between hydrazine and H_2O_2. The aptasensor demonstrates excellent performance in buffer and serum-added solutions,

Table 1 Comparative analysis of sensors prepared by different materials for cTnI detection

Material type	Sensor modifier	LOD (fg mL^{-1})	Detection range (fg mL^{-1})	References
Graphene-based composites	WO_3–RGO nanocomposite	—	$0.01–2.5 \times 10^8$	115
	CDs-3D-PG-Pd@Au NCs	33.3	—	116
Carbon nanotube-based composites	CNN and DNA aptamers	1.6×10^4	$2.4 \times 10^4–2.4 \times 10^{12}$	117
	AuNPs collaborates with Co_3O_4 to construct SWCNT FET	0.1×10^{12}	—	118
	Carboxyl-functionalized multi-walled carbon nanotubes	0.05×10^6	—	119
	CIL–HCNTs	6×10^3	$0.01–6.0 \times 10^7$	120
Graphene quantum dot composites	ABEI@GQDs	0.35	$1.0–5.0 \times 10^3$	121
	AuNCs-GQDs	3.542×10^2	$0.5 \times 10^3–2.0 \times 10^7$	122
	N–B-GQDs + Ce-SnO_2/SnS_2	2.00	—	123
Gold nanocomposites	C-dots@AuNP	—	—	124
	Au–CNN + GPRu-Au	3.94	$10.0–1.0 \times 10^7$	126
	Ab_2–AuNP–T_1 intelligent probe	1.01	$5.0–50 \times 10^6$	126
Polymetallic super-structured nanocrystals	PdCuPt/PPY/DCSC	16.03	$50.0–1.0 \times 10^9$	126
	Pd@PdPtCo MNPs	31	$1.0 \times 10^2–200 \times 10^6$	126
	PtCoCuPd HBTPs	0.2×10^3	$1.0 \times 10^3–1.0 \times 10^8$	126
Ceramic matrix composites	ZnO-NPs thin-film	0.324×10^3	—	126
	Fe_3O_4–NH_2 is loaded onto CoPc NPs	0.39×10^3	$1.0 \times 10^3–1.0 \times 10^8$	126
	IGZO	6.6×10^3	$1.0 \times 10^4–1.0 \times 10^9$	126
MOFs	Ab-NH_2-MIL-88B-(Fe_2Co)-MOF/NF	13	—	126
	N-ZIF-67@PBA	0.31	—	126
	RuMOFNSs	0.48	$1.0–1.0 \times 10^7$	126
	CNNS@NH_2-MIL(Fe)	0.38	—	126

with a dynamic range of 1–100 pM (0.024–2.4 ng mL^{-1}), a detection limit of 1.0 pM (24 pg mL^{-1}, below existing cutoff values), and high specificity for cTnI. This portable SPCE aptasensor is promising as an innovative diagnostic tool for AMI.

To enhance the ability to resist interference from interfering substances, Anthony P. O'Mullane *et al.*[47] developed a novel electrochemical immunosensor for the selective affinity binding and rapid detection of cTnI in plasma. The method involves depositing a PDATT conductive film on an ITO electrode *via* chronoamperometry, linking anti-cTnI antibodies through amide bonds, and backfilling gaps with BSA to minimize non-specific binding. Using DPV method, a peak at 0.27 V enables cTnI detection with a response range of 0.01–100 ng mL^{-1} and a quantification limit of 0.01 ng mL^{-1}. The sensor specifically detects cTnI in spiked plasma without interference from cTnT, achieving results in under 15 minutes, making it suitable for pathological laboratories and point-of-care testing.

In the development of high-performance electrochemical biosensors for troponin I (cTnI) detection, multi-component material systems serve as key breakthroughs (Table 1). Carbon-based materials, with their excellent electrical conductivity and large specific surface area, form a stable framework for sensors. However, their hydrophobicity hinders biomolecule immobilization, which can be improved by grafting hydrophilic groups through surface modification. Metal-based composites significantly enhance electron transfer efficiency and detection sensitivity, but are prone to oxidation and deactivation. Surface coating or alloying treatments effectively enhance their stability. Ceramic-based composites precisely regulate the microenvironment to ensure efficient chemical reactions, yet their high processing difficulty and costs can be addressed *via* novel preparation processes and large-scale production. Metal–organic framework (MOF) composites, with unique porous structures and customizable surfaces, show great potential in molecular recognition, though their stability is suboptimal. Post-modification or composite reinforcement can optimize their performance. Conductive polymer materials combined with electrochemical nanomarkers provide innovative detection solutions. Despite conductivity decay issues, doping modification and structural optimization extend their service life. These materials collaborate innovatively to continuously break through technical bottlenecks, propelling cTnI detection to new heights.

7. Conclusions

Currently, CVD is the leading condition that threatens global human health. As one of the most dangerous diseases, early and accurate diagnosis of AMI is crucial for reducing mortality and improving prognosis.[140–144] Among the numerous diagnostic indicators, cTnI is an important biomarker for diagnosing acute myocardial infarction because of its high specificity and sensitivity to acute myocardial cell injury. Against this backdrop, electrochemical biosensors have rapidly evolved as a highly promising technical means in the field of cTnI detection, with their unique benefits including high sensitivity, specificity, fast response, ease of operation, low cost, and miniaturization.

New sensing materials and detection technologies will continue to emerge with the rapid development of material science, nanotechnology, and biotechnology. The development

of new materials with high sensitivity, high specificity, and good stability will improve the performance of electrochemical biology sensors and achieve ultra-trace detection of cTnI. For instance, accurate identification and efficient detection of cTnI can be achieved by designing and synthesizing nanomaterials with specific structures and functions. Regarding detection equipment, miniaturization and the intelligence of detection equipment as well as deep integration with clinical sample processing and data management systems will significantly improve the diagnostic efficiency of CVD, and buy valuable time for clinical treatment. This is with the help of advanced surface modification techniques and signal processing algorithms to improve the anti-interference capacity of sensors and ensure the reliability of detection results. It can be broadly used in scenarios including home health monitoring and primary medical care.[145–149]

Looking ahead, the development trend of electrochemical biosensors for detecting cTnI shows a distinct trend of deep integration with artificial intelligence and wearable devices. AI technology can conduct comprehensive analysis and accurate processing of the massive and complex data generated by electrochemical biosensors. By mining and analyzing the detection data, precise quantitative detection and diagnosis of cTnI can be achieved, and the performance of the sensor can be continuously optimized with the help of machine learning algorithms based on colossal experimental data and actual detection feedback. This further improves the sensitivity and specificity of the detection, making the detection results more reliable.

Real-time, continuous monitoring by wearable devices revolutionizes health management and provides a convenient experience.[140,150] The integration of electrochemical biosensors makes it small and portable, allowing users to monitor key health indicators in their daily lives, detect changes in cTnI promptly, and capture potential health risks.[151–156] This cross-domain integration is important in the healthcare field. From a clinical perspective, real-time and accurate cTnI test data can help in the early detection of cardiovascular diseases, the development of more targeted and personalized treatment plans, as well as improvement of treatment outcomes. For the general public, it provides a convenient means of health monitoring and encourages active health awareness. However, the integration of the two faces many technical shortcomings, including the stability of long-term use of sensors, data transmission and processing accuracy, and information security protection. These challenges are gradually being resolved with the development of material science, nanotechnology, and information technology. The integration of electrochemical biosensors and wearable devices in the future is expected to bring about breakthroughs in CVD prevention and human health, as well as more opportunities for health management.[156,157]

Additionally, the involvement of multiple disciplines will inject new vitality into the development of electrochemical biosensors, enabling them to play a greater role in early diagnosis as well as precision treatment of CVD and driving continuous progress in the entire biomedical testing field.[100,158,159]

By achieving ultra-early and accurate detection of cTnI, doctors can timely identify CVD risks, and develop more targeted treatment plans at the nascent stage of the disease, effectively curbing the progression of the disease, and greatly improving patient prognosis. This will result in a qualitative leap in the prevention and treatment of CVD, as well as strongly promote the vigorous development of the entire biomedical field, making greater contributions to human health.

Data availability

This review does not contain any original research results, software or code, and as part of the review, no new data were generated or analyzed.

Author contributions

Ning Zhang provided the research methodology and revised the manuscript. Yuxin Zhu wrote the main body of the manuscript. Fachuang Li and Yusong Wang completed all the figures. Zheng Fu prepared all the tables in the manuscript. Mengda Jia, Xiaoran Zhan and Wanqing Zhang proofread all the figures, tables, and content. All authors reviewed the manuscript.

Conflicts of interest

The authors declare no competing interests.

Acknowledgements

This work was financially supported by the Key Scientific and Technological Project of Henan Province (No. 252102111060). We would like to thank all the reviews who participated in the reviewer and MJEditor (**https://www.mjeditor.com/**) for its linguistic assistance during the preparation of this manuscript.

References

1 M. Abdorahim, M. Rabiee, S. N. Alhosseini, M. Tahriri, S. Yazdanpanah, S. H. Alavi and L. Tayebi, *TrAC, Trends Anal. Chem.*, 2016, **82**, 337–347.
2 K. Kim, C. Park, D. Kwon, D. Kim, M. Meyyappan, S. Jeon and J.-S. Lee, *Biosens. Bioelectron.*, 2016, **77**, 695–701.
3 A. Nezami, S. Dehghani, R. Nosrati, N. Eskandari, S. M. Taghdisi and G. Karimi, *J. Pharm. Biomed. Anal.*, 2018, **159**, 425–436.
4 A. Nsabimana, X. Ma, F. Yuan, F. Du, A. Abdussalam, B. Lou and G. Xu, *Electroanalysis*, 2018, **31**, 177–187.
5 B. Regan, F. Boyle, R. O'Kennedy and D. Collins, *Sensors*, 2019, **19**, 3485.
6 S. Szunerits, V. Mishyn, I. Grabowska and R. Boukherroub, *Biosens. Bioelectron.*, 2019, **131**, 287–298.
7 G.-R. Han and M.-G. Kim, *Sensors*, 2020, **20**, 2593.

8 S.-S. Shan, S.-Y. Lu, Y.-P. Yang, S.-P. Lin, P. Carey, M. Xian, F. Ren, S. Pearton, C.-W. Chang, J. Lin and Y.-T. Liao, *IEEE Trans. Biomed. Circuits Syst.*, 2020, **14**, 1362–1370.
9 V. Mani, C. Durmus, W. Khushaim, D. C. Ferreira, S. Timur, F. Arduini and K. N. Salama, *Biosens. Bioelectron.*, 2022, **216**, 114680.
10 L. Tang, J. Yang, Y. Wang and R. Deng, *ACS Sens.*, 2023, **8**, 956–973.
11 S. Zhong, L. Chen, X. Shi, G. Chen, D. Sun and L. Zhang, *Microchem. J.*, 2023, **193**, 109063.
12 R. Devaraj, A. K. Loganathan and L. Krishnamoorthy, *Heliyon*, 2024, **10**, e33238.
13 M. J. Saadh, F. A. Muhammad, R. J. Albadr, A. K. Bishoyi, S. Ballal, L. Bareja, K. S. Naidu, J. Rizaev, W. M. Taher, M. Alwan, M. J. Jawad and A. M. Ali Al-Nuaimi, *Clin. Chim. Acta*, 2025, **567**, 120094.
14 M. Jiang, Y. Wang, W. Yuan, H. Li, Y. Jin, W. Yan, X. Ze, K. Kang, L. Jia, L. You and L. Niu, *Sens. Actuators, B*, 2025, **423**, 136794.
15 S. Zhang, L. Chen, Y. Tan, S. Wu, P. Guo, X. Jiang and H. Pan, *Anal. Methods*, 2024, **16**, 6715–6725.
16 L. Zeng, C. Lin, P. Liu, D. Sun and J. Lu, *Chem. Eng. J.*, 2023, **474**, 145525.
17 Y. Wang, R. Singh, S. Chaudhary, B. Zhang and S. Kumar, *IEEE Trans. Instrum. Meas.*, 2022, **71**, 1–9.
18 J. Wang, D. Chen, W. Huang, N. Yang, Q. Yuan and Y. Yang, *Exploration*, 2023, **3**, 20210027.
19 X. Liu, Q. Li, W. Chen, P. Shen, Y. Sun, Q. Chen, J. Wu, J. Zhang, P. Lu, H. Lin, X. Tang and P. Gao, *Fundam. Res.*, 2021, **1**, 534–542.
20 X. Qin, D. Li, X. Qin, F. Chen, H. Guo, Y. Gui, J. Zhao, L. Jiang and D. Luo, *View*, 2024, **5**, 20240025.
21 T. Wang, H.-S. Tan, L.-X. Zhao, M. Liu and S.-S. Li, *Sens. Actuators, B*, 2024, **412**, 135804.
22 S. Wang, J. Qin, Y. Liang, Y. Ye, S. Li, Y. Guo, X. Yang and Y. Liang, *Microchem. J.*, 2024, **196**, 109610.
23 Q. Yang, Y. Hao, Z. Chen, N. Lan, X. He, D. Hu, Z. Xu, L. Liang, D. Cao, J. Guo, Y. Ran and B.-O. Guan, *Sens. Actuators, B*, 2023, **393**, 134248.
24 S. Wang, J. Qin, Y. Liang, Y. Ye, Y. Guo, S. Li, X. Yang and Y. Liang, *Anal. Chim. Acta*, 2024, **1332**, 343316.
25 J. Li, Y. Lv, N. Li, R. Wu, J. Li, J. You, H. Shen, X. Chen and L. S. Li, *Sens. Actuators, B*, 2021, **344**, 130275.
26 G. Zhang, L. Zhang, Y. Yu, B. Lin, Y. Wang, M. Guo and Y. Cao, *Biosens. Bioelectron.*, 2020, **167**, 112502.
27 D. Tu, A. Holderby and G. L. Coté, *J. Biomed. Opt.*, 2020, **25**, 097001.
28 F. Chen, Q. Wu, D. Song, X. Wang, P. Ma and Y. Sun, *Colloids Surf., B*, 2019, **177**, 105–111.
29 V. Baldoneschi, P. Palladino, M. Banchini, M. Minunni and S. Scarano, *Biosens. Bioelectron.*, 2020, **157**, 112161.
30 D. Çimen, N. Bereli, S. Günaydın and A. Denizli, *Talanta*, 2020, **219**, 121259.
31 R. K. Sinha, *Sens. Actuators, A*, 2021, **332**, 113104.
32 Y. Hua, R. Wang and D. Li, *Micromachines*, 2022, **13**, 1036.
33 S. Choudhary and Z. Altintas, *Biosensors*, 2023, **13**, 229.
34 Y. Wang, R. Singh, M. Li, R. Min, Q. Wu, B. K. Kaushik, R. Jha, B. Zhang and S. Kumar, *IEEE Trans. Nanobiosci.*, 2023, **22**, 375–382.
35 R. S. Alves, F. A. Sigoli and I. O. Mazali, *Nanotechnology*, 2020, **31**, 505505.
36 A. Sharma, A. I. Y. Tok, C. Lee, R. Ganapathy, P. Alagappan and B. Liedberg, *Sens. Actuators, B*, 2019, **285**, 431–437.
37 G.-R. Han, H. J. Koo, H. Ki and M.-G. Kim, *ACS Appl. Mater. Interfaces*, 2020, **12**, 34564–34575.
38 R. Nie, J. Huang, X. Xu and L. Yang, *Anal. Chem.*, 2020, **92**, 6257–6262.
39 S. Nisar, Chansi, A. Mathur, T. Basu, K. R. B. Singh and J. Singh, *Biosensors*, 2022, **12**, 1144.
40 T. A. Tabish, H. Hayat, A. Abbas and R. J. Narayan, *Biosensors*, 2022, **12**, 77.
41 G. K. Hasabnis and Z. Altintas, *ACS Omega*, 2024, **9**, 30737–30750.
42 W. Kim, S. Lee and S. Jeon, *Sens. Actuators, B*, 2018, **273**, 1323–1327.
43 T. Liu, L.-L. Liang, P. Xiao, L.-P. Sun, Y.-Y. Huang, Y. Ran, L. Jin and B.-O. Guan, *Biosens. Bioelectron.*, 2018, **100**, 155–160.
44 X. Fu, Y. Wang, Y. Liu, H. Liu, L. Fu, J. Wen, J. Li, P. Wei and L. Chen, *Analyst*, 2019, **144**, 1582–1589.
45 S. Palanisamy, D. Senthil Raja, B. Subramani, T.-H. Wu and Y.-M. Wang, *ACS Appl. Mater. Interfaces*, 2020, **12**, 32468–32476.
46 S.-Y. Cen, X.-Y. Ge, Y. Chen, A.-J. Wang and J.-J. Feng, *Microchem. J.*, 2021, **169**, 106568.
47 M. D. Gholami, A. P. O'Mullane, P. Sonar, G. A. Ayoko and E. L. Izake, *Anal. Chim. Acta*, 2021, **1185**, 339082.
48 H. Zhao, L. Cao, Q. Liu, F. Tang, L. Chen, S. Wang, Y. Li, Y. Li, B. Li and H. Liu, *Sens. Actuators, B*, 2022, **351**, 130970.
49 Y. Huang, Y. Zhang, J. Lv, Y. Shao, D. Yang and Y. Cong, *Nanoscale Adv.*, 2023, **5**, 830–839.
50 Z. Mokhtari, S. Hashemnia, H. Khajehsharifi and S. Noroozi, *Mater. Today Chem.*, 2023, **30**, 101588.
51 C. Tang, C.-L. Lv, P. Chen, A.-J. Wang, J.-J. Feng, T. Yun Cheang and H. Xia, *Bioelectrochemistry*, 2024, **157**, 108639.
52 R. Adzhri, M. K. Md Arshad, S. C. B. Gopinath, A. R. Ruslinda, M. F. M. Fathil, C. Ibau and M. N. M. N., *Sens. Actuators, A*, 2017, **259**, 57–67.
53 I. Sarangadharan, A. Regmi, Y.-W. Chen, C.-P. Hsu, P.-c. Chen, W.-H. Chang, G.-Y. Lee, J.-I. Chyi, S.-C. Shiesh, G.-B. Lee and Y.-L. Wang, *Biosens. Bioelectron.*, 2018, **100**, 282–289.
54 I. Sarangadharan, S.-L. Wang, R. Sukesan, P.-c. Chen, T.-Y. Dai, A. K. Pulikkathodi, C.-P. Hsu, H.-H. K. Chiang, L. Y.-M. Liu and Y.-L. Wang, *Anal. Chem.*, 2018, **90**, 2867–2874.
55 J. Li, Y. Kutovyi, I. Zadorozhnyi, N. Boichuk and S. Vitusevich, *Adv. Mater. Interfaces*, 2020, **7**, 2000508.
56 T.-M. Pan, C.-W. Wang, W.-C. Weng, C.-C. Lai, Y.-Y. Lu, C.-Y. Wang, I. C. Hsieh and M.-S. Wen, *Biosens. Bioelectron.*, 2022, **201**, 113977.
57 K.-W. Wong, D. Xu, D. He, M. S. Wong and H.-W. Li, *Sens. Actuators, B*, 2019, **291**, 200–206.

58 Z. Wang, H. Zhao, K. Chen, H. Li and M. Lan, *Anal. Chim. Acta*, 2021, **1188**, 339202.
59 J. Liu, G. Ruan, W. Ma, Y. Sun, H. Yu, Z. Xu, C. Yu, H. Li, C.-w. Zhang and L. Li, *Biosens. Bioelectron.*, 2022, **198**, 113823.
60 Z. Song, J. Song, F. Gao, X. Chen, Q. Wang, Y. Zhao, X. Huang, C. Yang and Q. Wang, *Sens. Actuators, B*, 2022, **368**, 132205.
61 S. N. Eshlaghi, L. Syedmoradi, A. Amini and K. Omidfar, *IEEE Sens. J.*, 2023, **23**, 3439–3445.
62 S. Kakkar, S. Chauhan, Bharti, M. Rohit and V. Bhalla, *Bioelectrochemistry*, 2023, **150**, 108348.
63 C. Li, H. Yang, Z. Song, F. Gao, L. Niu and Q. Wang, *Sens. Actuators, B*, 2024, **411**, 135746.
64 Y. Xue, R. Shi, L. Chen, S. Ju, T. Yan, X. Tan, L. Hou, L. Jin and B. Shen, *Langmuir*, 2024, **40**, 26988–26996.
65 S.-N. Qin, Y.-C. Nong, C.-L. Cao, L.-Y. Chen, Y.-J. Cao, T. Wan, L. Feng, K. Salminen, J.-J. Sun and J. Li, *Talanta*, 2025, **284**, 127250.
66 C. Bao, X. Liu, X. Shao, X. Ren, Y. Zhang, X. Sun, D. Fan, Q. Wei and H. Ju, *Biosens. Bioelectron.*, 2020, **157**, 112157.
67 Y. Xue, Y. Han, H. Xia, Y. Fan, C. Peng, H. Xing, J. Li and E. Wang, *ChemElectroChem*, 2020, **7**, 4343–4348.
68 J.-T. Cao, L.-Z. Zhao, Y.-Z. Fu, X.-M. Liu, S.-W. Ren and Y.-M. Liu, *Sens. Actuators, B*, 2021, **331**, 129427.
69 H. Dong, Z. Wu, S. Liu, Y. Li, F. Jiang, Q. Liu, P. Wang, Z. Xu and Y. Li, *Talanta*, 2022, **249**, 123649.
70 P. Li, S. Lin, Z. Zheng, J. Yang, Z. Lin, D. Zheng, L. Huang, Y. Chen and W. Gao, *Sens. Actuators, B*, 2022, **357**, 131439.
71 H.-J. Li, Y. Huang, S. Zhang, C. Chen, X. Guo, L. Xu, Q. Liao, J. Xu, M. Zhu, X. Wang, D. Wang and B. He, *ACS Sens.*, 2023, **8**, 2030–2040.
72 J. Guo, G. Kuang, D. Luo, W. Yu, L. Chen and Y. Fu, *Talanta*, 2024, **277**, 126342.
73 R. Memon, I. Shaheen, A. Qureshi and J. H. Niazi, *J. Alloys Compd.*, 2024, **1008**, 176592.
74 Z.-Z. Xu, B.-F. Xu, A. P. Tanjung, L. Zhang, A.-J. Wang, P. Song, L.-P. Mei and J.-J. Feng, *Sens. Actuators, B*, 2024, **412**, 135732.
75 S. Zhang, C. Mao, H. Wang, M. Gao and L. Zhao, *Chem. Eng. J.*, 2024, **502**, 157966.
76 V. Mishyn, T. Rodrigues, Y. R. Leroux, L. Butruille, E. Woitrain, D. Montaigne, P. Aspermair, H. Happy, W. Knoll, R. Boukherroub and S. Szunerits, *Anal. Bioanal. Chem.*, 2021, **414**, 5319–5327.
77 S. He, P. Zhang, J. Sun, Y. Ji, C. Huang and N. Jia, *Biosens. Bioelectron.*, 2022, **201**, 113962.
78 L. Huang, G. Cai, R. Zeng, Z. Yu and D. Tang, *Anal. Chem.*, 2022, **94**, 9487–9495.
79 Z. Yu, H. Gong, J. Xu, Y. Li, F. Xue, Y. Zeng, X. Liu and D. Tang, *Anal. Chem.*, 2022, **94**, 7408–7416.
80 H. Zhao, J. Zheng, H. Liang, H.-F. Liu, F. Liu, Y.-P. Zhang and C.-P. Li, *Sens. Actuators, B*, 2023, **391**, 134026.
81 N. Singh, A. Kaushik, I. Ghori, P. Rai, L. Dong, A. Sharma, B. D. Malhotra and R. John, *ACS Appl. Mater. Interfaces*, 2024, **16**, 32794–32811.
82 D. Bhatnagar, I. Kaur and A. Kumar, *Int. J. Biol. Macromol.*, 2017, **95**, 505–510.
83 E. Spain, S. Carrara, K. Adamson, H. Ma, R. O'Kennedy, L. De Cola and R. J. Forster, *ACS Omega*, 2018, **3**, 17116–17124.
84 M. Lakshmanakumar, N. Nesakumar, S. Sethuraman, K. S. Rajan, U. M. Krishnan and J. B. B. Rayappan, *Sci. Rep.*, 2019, **9**, 17348.
85 B. D. Mansuriya and Z. Altintas, *Nanomaterials*, 2021, **11**, 2525.
86 Z. Guo, X. Zhao, Y. Zhou, Y. Li, Z. Liu, M. Luo, X. Wu, Y. Wang, M. Zhang and X. Yang, *J. Biophot.*, 2022, **15**, e202200151.
87 M. Vasudevan, S. Remesh, V. Perumal, P. B. Raja, M. N. M. Ibrahim, S. C. B. Gopinath, H.-L. Lee, S. Karuppanan, M. Ovinis, N. Arumugam and R. S. Kumar, *Microchem. J.*, 2023, **195**, 109405.
88 J. N. Chen, G. K. Hasabnis, E. Akin, G. Gao, S. P. Usha, R. Süssmuth and Z. Altintas, *Sens. Actuators, B*, 2024, **417**, 136052.
89 R. Tannenberg, M. Paul, B. Röder, S. L. Gande, S. Sreeramulu, K. Saxena, C. Richter, H. Schwalbe, C. Swart and M. G. Weller, *Biosensors*, 2023, **13**, 455.
90 Z. Yu, Q. Lin, H. Gong, M. Li and D. Tang, *Biosens. Bioelectron.*, 2023, **223**, 115028.
91 X. Du, W. Zhang, S. Yi, S. Li, H. Li and F. Xia, *Langmuir*, 2024, **40**, 18214–18224, DOI: **10.1021/acs.langmuir.4c01979**.
92 J. Zhang, K. Sun, J. Ren, H. Wang and J. Cheng, *Sens. Actuators, B*, 2024, **401**, 135001.
93 X. Mi, H. Li, R. Tan, B. Feng and Y. Tu, *Biosens. Bioelectron.*, 2021, **192**, 113482.
94 H.-J. Li, S. Zhi, S. Zhang, X. Guo, Y. Huang, L. Xu, X. Wang, D. Wang, M. Zhu and B. He, *Biomater. Sci.*, 2022, **10**, 4627–4634.
95 B. Wang, C. Wang, Y. Li, X. Liu, D. Wu and Q. Wei, *Analyst*, 2022, **147**, 4768–4776.
96 K. Chen, H. Zhao, Z. Wang, F. Zhou and M. Lan, *Sens. Actuators, B*, 2023, **390**, 134044.
97 W. Guo, J. Wang, W. Guo, Q. Kang and F. Zhou, *Anal. Bioanal. Chem.*, 2021, **413**, 4847–4854.
98 J. Li, S. Zhang, L. Zhang, Y. Zhang, H. Zhang, C. Zhang, X. Xuan, M. Wang, J. Zhang and Y. Yuan, *Front. Chem.*, 2021, **9**, 680593.
99 S. Dudala, S. K. Dubey, A. Javed, A. Ganguly and S. Goel, *J. Micromech. Microeng.*, 2022, **32**, 104001.
100 P. Niu, J. Jiang, K. Liu, S. Wang, T. Wang, Y. Liu, X. Zhang, Z. Ding and T. Liu, *Nanophotonics*, 2022, **11**, 3351–3364.
101 A. V. Orlov, J. A. Malkerov, D. O. Novichikhin, S. L. Znoyko and P. I. Nikitin, *Int. J. Mol. Sci.*, 2022, **23**, 4474.
102 K. Toma, K. Oishi, K. Iitani, T. Arakawa and K. Mitsubayashi, *Sens. Actuators, B*, 2022, **368**, 132132.
103 S. Varghese, A. S. Madanan, M. K. Abraham, A. I. Shkhair, G. Indongo, G. Rajeevan, N. S. Vijila and S. George, *Microchem. J.*, 2023, **194**, 109327.
104 D. Wu, Q. Zhao, J. Sun and X. Yang, *Chin. Chem. Lett.*, 2023, **34**, 107672.

105 I. Lopez Carrasco, G. Cuniberti, J. Opitz and N. Beshchasna, *Biosensors*, 2024, **14**, 341.
106 H. Yang, S. Zhu, L. Pang, Y. Ma, X. Liu and J. Liu, *Sens. Actuators, B*, 2024, **406**, 135388.
107 Y. Ma, X.-L. Shen, H.-S. Wang, J. Tao, J.-Z. Huang, Q. Zeng and L.-S. Wang, *Anal. Biochem.*, 2017, **520**, 9–15.
108 G. Shen and Y. Shen, *ACS Omega*, 2019, **4**, 20252–20256.
109 Q. Shen, M. Liu, Y. Lü, D. Zhang, Z. Cheng, Y. Liu, H. Gao and Z. Jin, *ACS Omega*, 2019, **4**, 11888–11892.
110 A. Quijano-Rubio, H.-W. Yeh, J. Park, H. Lee, R. A. Langan, S. E. Boyken, M. J. Lajoie, L. Cao, C. M. Chow, M. C. Miranda, J. Wi, H. J. Hong, L. Stewart, B.-H. Oh and D. Baker, *Nature*, 2021, **591**, 482–487.
111 Y. Liu, R. Gao, Y. Zhuo, Y. Wang, H. Jia, X. Chen, Y. Lu, D. Zhang and L. Yu, *Anal. Chim. Acta*, 2023, 1239.
112 W. Ma, L. Pang, J. Liu, L. Wen, H. Ma, Y. Li, Z. Xu, C. Zhang and H.-D. Yu, *Anal. Chem.*, 2023, **95**, 6323–6331.
113 A. Ibrahim Shkhair, A. S. Madanan, S. Varghese, M. K. Abraham, G. Indongo, G. Rajeevan, B. K. Arathy, S. Muneer Abbas and S. George, *Chem.–Eur. J.*, 2024, **30**, e202401867.
114 G. Liu, M. Chen, J. Wang, X. Cui, K. Wang, Z. Yang, A. Gao, A. Zhang, Q. Zhang, Y. Shen, G. Gao and D. Cui, *Sens. Actuators, B*, 2024, **414**, 135921.
115 D. Sandil, S. Srivastava, B. D. Malhotra, S. C. Sharma and N. K. Puri, *J. Alloys Compd.*, 2018, **763**, 102–110.
116 X. Zhang, H. Lv, Y. Li, C. Zhang, P. Wang, Q. Liu, B. Ai, Z. Xu and Z. Zhao, *J. Mater. Chem. B*, 2019, **7**, 1460–1468.
117 G. Park, H. Lee, M. Jang, J. A. Park, H. Park, C. Park, T.-H. Kim, M.-H. Lee and T. Lee, *Sens. Actuators, B*, 2023, **393**, 134295.
118 S. G. Surya, S. M. Majhi, D. K. Agarwal, A. A. Lahcen, S. Yuvaraja, K. N. Chappanda and K. N. Salama, *J. Mater. Chem. B*, 2020, **8**, 18–26.
119 S. Vasantham, R. Alhans, C. Singhal, S. Nagabooshanam, S. Nissar, T. Basu, S. C. Ray, S. Wadhwa, J. Narang and A. Mathur, *Biomed. Microdevices*, 2019, **22**, 6.
120 H. Yan, X. Tang, X. Zhu, Y. Zeng, X. Lu, Z. Yin, Y. Lu, Y. Yang and L. Li, *Sens. Actuators, B*, 2018, **277**, 234–240.
121 M. Guo, J. Shu, D. Du, M. A. Haghighatbin, D. Yang, Z. Bian and H. Cui, *Sens. Actuators, B*, 2021, **334**, 129628.
122 O. Karaman, N. Özcan, C. Karaman, B. B. Yola, N. Atar and M. L. Yola, *Mater. Today Chem.*, 2022, **23**, 100666.
123 Z. Wu, S. Liu, Y. Li, F. Tang, Z. Zhao, Q. Liu, Y. Li and Q. Wei, *Sens. Actuators, B*, 2021, **336**, 129733.
124 X. Qin, Y. Dong, M. Wang, Z. Zhu, M. Li, X. Chen, D. Yang and Y. Shao, *Sci. China: Chem.*, 2018, **61**, 476–482.
125 H. Hui, S. C. B. Gopinath, Z. H. Ismail, Y. Chen, K. Pandian, Y. Velusamy, D. Yang and Y. Shao, *Biotechnol. Appl. Biochem.*, 2022, **70**, 581–591.
126 L. Zhu, J. Ye, M. Yan, Q. Zhu, S. Wang, J. Huang and X. Yang, *ACS Sens.*, 2019, **4**, 2778–2785.
127 M. Wang, H.-N. Sun, X.-Y. Liu, M. Liu and S.-S. Li, *Bioelectrochemistry*, 2025, **161**, 108838.
128 Y. Chen, L.-P. Mei, J.-J. Feng, P.-X. Yuan, X. Luo and A.-J. Wang, *Biosens. Bioelectron.*, 2019, **145**, 111638.
129 N. Radha Shanmugam, S. Muthukumar, S. Chaudhry, J. Anguiano and S. Prasad, *Biosens. Bioelectron.*, 2017, **89**, 764–772.
130 M. F. M. Fathil, M. K. Md Arshad, A. R. Ruslinda, S. C. B. Gopinath, M. M. N. Nuzaihan, R. Adzhri, U. Hashim and H. Y. Lam, *Sens. Actuators, B*, 2017, **242**, 1142–1154.
131 J. Y. Lim and S. S. Lee, *Talanta*, 2021, **228**, 122233.
132 Y. F. Shi, Y. P. Jiang, X. Z. Wang, Z. Q. Zhang, J. Z. Huo, Y. Y. Liu, X. R. Wang and B. Ding, *ACS Appl. Nano Mater.*, 2022, **5**, 15629–15641.
133 N. Ma, T. Zhang, T. Yan, X. Kuang, H. Wang, D. Wu and Q. Wei, *Biosens. Bioelectron.*, 2019, **143**, 111608.
134 W. Khushaim, M. T. Vijjapu, S. Yuvaraja, V. Mani and K. N. Salama, *Biosensors*, 2022, **12**, 386.
135 X. Peng, R. Xu, F. Yu, J. Xu, Y. Wang and S. Wang, *Talanta*, 2025, **283**, 127177.
136 M. Yan, J. Ye, Q. Zhu, L. Zhu, J. Huang and X. Yang, *Anal. Chem.*, 2019, **91**, 10156–10163.
137 J. Zhao, J. Du, J. Luo, S. Chen and R. Yuan, *Sens. Actuators, B*, 2020, **311**, 127934.
138 J. Zuo, X. Zhao, X. Ju, S. Qiu, W. Hu, T. Fan and J. Zhang, *Electroanalysis*, 2016, **28**, 2044–2049.
139 H. Jo, J. Her, H. Lee, Y.-B. Shim and C. Ban, *Talanta*, 2017, **165**, 442–448.
140 K. Alsabbagh, T. Hornung, A. Voigt, S. Sadir, T. Rajabi and K. Länge, *Biosensors*, 2021, **11**, 80.
141 F. Geng, X. Liu, T. Wei, Z. Wang, J. Liu, C. Shao, G. Liu, M. Xu and L. Feng, *Sens. Actuators, B*, 2023, **378**, 133121.
142 P. P. Goswami, T. Deshpande, D. R. Rotake and S. G. Singh, *Biosens. Bioelectron.*, 2023, **220**, 114915.
143 G.-R. Han, A. Goncharov, M. Eryilmaz, H.-A. Joung, R. Ghosh, G. Yim, N. Chang, M. Kim, K. Ngo, M. Veszpremi, K. Liao, O. B. Garner, D. Di Carlo and A. Ozcan, *ACS Nano*, 2024, **18**, 27933–27948.
144 X. Hu, J. Li, Y.-T. Li, Y. Zhang, M.-M. Xiao, Z. Zhang, Y. Liu, Z.-Y. Zhang and G.-J. Zhang, *Biosens. Bioelectron.*, 2024, **246**, 115909.
145 H. Bai, L. He, J.-H. Liu, Z.-J. Liu, J.-T. Ren and E.-K. Wang, *Chin. J. Anal. Chem.*, 2023, **51**, 100190.
146 J. Chen, X. Sun, Y. Wang, Z. Gao and B. Zheng, *Sens. Actuators, B*, 2023, **385**, 133712.
147 M. K. Abraham, A. S. Madanan, S. Varghese, A. I. Shkhair, G. Indongo, G. Rajeevan, N. S. Vijila and S. George, *Analyst*, 2024, **149**, 231–243.
148 S. M. Anju, K. A. Merin, S. Varghese, A. I. Shkhair, G. Rajeevan, G. Indongo and S. George, *Microchim. Acta*, 2024, **191**, 124.
149 B. Bao, X. Tian, R. Wang and D. Li, *Sens. Actuators, B*, 2024, **415**, 135989.
150 D. K. Agarwal, A. Kushagra, M. Ashwin, A. S. Shukla and V. Palaparthy, *Nanotechnology*, 2020, **31**, 115503.
151 C. Liang, Y. Liu, C. Liu, X. Li, L. Chen, C. Duan and J. Li, *Sens. Actuators, B*, 2018, **273**, 1508–1518.
152 A. Sinha, P. Gopinathan, Y.-D. Chung, H.-Y. Lin, K.-H. Li, H.-P. Ma, P.-C. Huang, S.-C. Shiesh and G.-B. Lee, *Biosens. Bioelectron.*, 2018, **122**, 104–112.

153 P. Gopinathan, A. Sinha, Y.-D. Chung, S.-C. Shiesh and G.-B. Lee, *Analyst*, 2019, **144**, 4943–4951.
154 L. Miao, L. Jiao, Q. Tang, H. Li, L. Zhang and Q. Wei, *Sens. Actuators, B*, 2019, **288**, 60–64.
155 A. Sinha, T.-Y. Tai, K.-H. Li, P. Gopinathan, Y.-D. Chung, I. Sarangadharan, H.-P. Ma, P.-C. Huang, S.-C. Shiesh, Y.-L. Wang and G.-B. Lee, *Biosens. Bioelectron.*, 2019, **129**, 155–163.
156 S. Boonkaew, I. Jang, E. Noviana, W. Siangproh, O. Chailapakul and C. S. Henry, *Sens. Actuators, B*, 2021, **330**, 129336.
157 K. Khachornsakkul and W. Dungchai, *ACS Sens.*, 2021, **6**, 1339–1347.
158 M. Xu, S. Li, M. Guan, Y. Zhang and Y. Zeng, *Appl. Phys. Express*, 2020, **13**, 021003.
159 X. Xiao, Z. Kuang, J. M. Slocik, S. Tadepalli, M. Brothers, S. Kim, P. A. Mirau, C. Butkus, B. L. Farmer, S. Singamaneni, C. K. Hall and R. R. Naik, *ACS Sens.*, 2018, **3**, 1024–1031.